

A Universal Framework to Construct a Huffman-Code-Mapping-based Reversible Data Hiding Scheme for JPEG Images

Abstract—Huffman code mapping (HCM) is a recent technique for reversible data hiding (RDH) in JPEG images. The existing HCM-based RDH schemes cause neither file-size increment nor visual distortion for the marked JPEG image, which is the superiority compared to the RDH schemes that use other techniques, such as histogram shifting (HS). However, the embedding capacity achieved by the HCM-based RDH schemes is much lower than the HS-based RDH schemes. Moreover, the existing HCM-based schemes are only applicable to the JPEG images coded with the default Huffman table. In this paper, we propose a universal framework to design the HCM-based RDH scheme. Under this framework, the key issue of HCM-based schemes, i.e., construct the optimal code mapping relationship, is converted to solve a combinatorial optimization problem. The high embedding capacity can be achieved with a slight increase in the file-size of the marked JPEG image. In addition, the problem of applicability is also solved by customizing the Huffman table. As a realization, we construct a new HCM-based scheme by employing the genetic algorithm to search the nearly optimal solution. Experiments show that the performance on the file-size preservation, visual quality, and computational complexity is superior to recent HS-based RDH schemes under the identical payload.

Index Terms—Reversible data hiding (RDH), JPEG, Huffman coding mapping (HCM), genetic algorithm (GA).

I. INTRODUCTION

REVERSIBLE data hiding (RDH) is a branch of data hiding technology, which can embed additional data into cover media imperceptibly, and the cover media can be restored losslessly. The reversibility is necessary for many applications, e.g., medical image processing and multimedia management. In the past decade, many RDH schemes for uncompressed images are designed. The existing RDH schemes are mainly based on three categories techniques: 1) lossless compression [1] [2], 2) difference expansion (DE) [3] [4], and 3) histogram shifting (HS) [5]–[8]. However, the compressed images are more widely used on the Internet, benefit from the low cost for storage or transmission. As JPEG is the most commonly used compression image format, developing the RDH schemes for JPEG images is required.

Recently, quite some RDH schemes for JPEG images have been proposed. According to the modification objects, the existing RDH schemes for JPEG images can be divided into two categories. The first category of schemes [9]–[20] is based on modifying the Discrete Cosine Transform (DCT) coefficients. The second category of schemes [21]–[24] is based on modifying the Huffman codes.

Since the DCT coefficients and the pixels are all integers, most of the techniques used in the first category of RDH in JPEG images are derived from the techniques designed for uncompressed images. For instance, some early works [9] [10]

are proposed to embed data by modifying the quantization table while modifying the DCT coefficients. In essence, the techniques adopted in [9] [10] is the DE technique. The lossless compression for DCT coefficients is introduced in [11], which is proposed by Fridrich *et al.*. In [11], additional data is embedded into a vacated room created by compressing the LSBs of non-zero alternating current (AC) coefficients.

The HS technique can also be extended from uncompressed images to JPEG images. In addition, HS technique is the most popular technique for RDH in JPEG images since this type of schemes can keep good visual quality and also achieve a smaller file size increments. In early HS-based RDH schemes [12] [13] for JPEG images, a problem is modifying the AC coefficients that values of 0, which leads to a significant increase in the file-size inevitably. To address this problem, Huang *et al.* [14] proposed a new HS-based RDH scheme that keeps the zero AC coefficient unchanged and sets the AC coefficients that values of 1 and -1 as the peak points of the histogram. The variation of all non-zero AC coefficients is at most 1 so the visual quality is well preserved. Later, some improved works [15]–[17] based on Huang *et al.*'s scheme are proposed, which aim to further improve the capabilities of visual quality and file-size preservation. In 2020, He *et al.* [18] established a negative influence model to determine the frequency selection and defined a weighting factor to adjust the optimization objective of the provided scheme. Yin *et al.* [19] improved the prior HS-based methods by designing a multiple-objective optimization algorithm. Li *et al.* [20] proposed a scheme that constructs a new two-dimensional histogram for JPEG images and achieved well performance.

For the second category of RDH schemes, the used technique is a new reversible embedding technique based on the characteristic of the JPEG bitstream, which is referred to as Huffman code mapping (HCM). Qian and Zhang [21] proposed a file-size preserving HCM-based scheme. In [21], the used code is assigned with multiple unused codes with the same code lengths to construct a code mapping set. The JPEG file header is also modified to keep the visual quality unchanged. After that, some works [22]–[24] are proposed to improve the embedding capacity. In Hu *et al.*'s scheme [22], the capacity is improved by searching the optimal combination according to the frequency of codes. Then, Qiu *et al.* [23] proposed an alternative embedding method by reordering the codes to improve the capacity further. Later, Zhang *et al.* [24] improved the scheme further by enlarging the search space.

Compared to the HS-based RDH schemes, the explicit advantages of HCM-based RDH schemes are no visual distortion and no increase in the file-size of the marked JPEG image.

However, two problems existing in the HCM-based RDH schemes cannot be ignored. One is the quite lower embedding capacity than HS-based RDH schemes. The other one is the previous HCM-based schemes can only be applied to the JPEG images coded with the default Huffman table. Because the unused codes contained in the default Huffman table are necessary to construct the mapping relationship for the HCM technique. When there are no unused codes in a Huffman table, the previous HCM technique is unavailable.

Is it possible to construct an HCM-based RDH scheme that can be applied to the JPEG images coded with any Huffman table and achieve high embedding capacity while keeping visual quality with no distortion? In this paper, we positively answer this question by designing a universal framework to construct the HCM-based RDH scheme and proposing a new HCM-based RDH scheme as an example. The high embedding capacity can be achieved by mapping multiple codes to the high-frequency symbols in a Huffman table. Surely, the benefit of high embedding capacity cannot come for free. The cost is a slight file-size increment. In Section VI, we compare the file-size increment at identical payload with the recent HS-based schemes and find that the file-size increment caused by our proposed scheme is lower than HS-based schemes. The main contributions of this paper are summarized as follows:

- 1) A new code mapping strategy is adopted to convert the construction of the optimal code mapping relationship into a combinatorial optimization problem.
- 2) A universal framework to construct an HCM-based scheme is formally proposed. Under this framework, the key issue is to solve the optimization problem with different given constraints.
- 3) As a realization of the proposed framework, a new HCM-based RDH scheme for JPEG images is provided by employing the genetic algorithm (GA) with some problem-oriented designs to solve the optimization problem.

The remainder of this paper is organized as follows. Firstly, the encoding of AC coefficients in JPEG bitstream and the HCM-based RDH technique is introduced in Section II. Section III provided the motivation of this paper. Then, the new code mapping strategy and the universal framework based on it are presented in Section IV. Later, the proposed scheme is described in detail in Section V. In Section VI, experimental results and analysis are included. Finally, the conclusions are drawn in Section VII.

II. BACKGROUND

In this section, the encoding of AC coefficients in the JPEG bitstream is first introduced briefly. Then, the current HCM-based RDH schemes are reviewed.

A. Encoding of AC coefficients in JPEG Bitstream

In the entropy coding phase of JPEG standard, the quantized AC coefficients are first compressed by run length encoding (RLE) into the form of $(run/size, value)$. $value$ is the amplitude of the next nonzero AC coefficient, which is coded by variable length integer (VLI) encoding and the generated codes are referred to as appended bits. $run(0 \leq run \leq 15)$ represents

the number of zero AC coefficients before the next nonzero AC coefficient. $size(1 \leq size \leq 10)$ denotes the code length needed to represent $value$. The symbol $run/size$, which is referred to as to Run/Size Value (RSV) throughout the paper, is encoded with Huffman coding for further compression. Finally, the entropy coded data and other information used to encode and decode are stored in the form of bitstream.

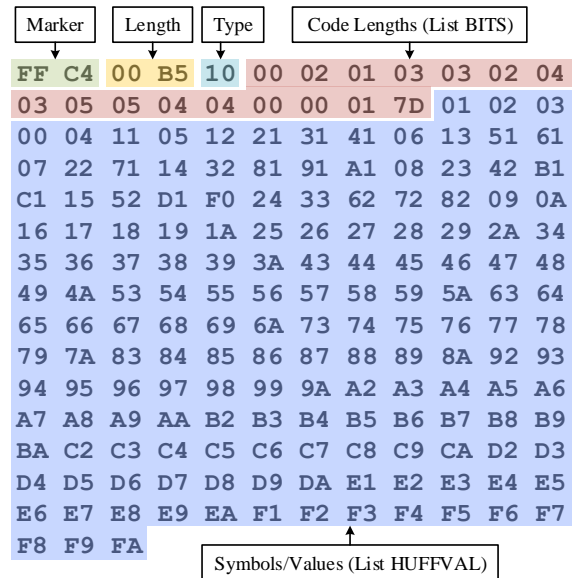


Fig. 1. The Structure of the DHT Segment for AC coefficients.

In JPEG bitstream, only the RSVs and the lengths of the codes assigned to each RSV are recorded in the define Huffman table (DHT) segment of the JPEG header, instead of the Huffman codes. The DHT segment includes two lists, BITS and HUFFVAL, which is provided in Fig. 1. As shown in Fig. 1, $0xFFC4$ is the marker represents the DHT segment and $0x00B5$ is the segment length except for the marker $0xFFC4$. The list BITS contains the number of codes of different lengths, which occupies 16 bytes totally, i.e., the number of codes of length i occupies one byte. The list HUFFVAL contains the symbols/RSVs, which is the hexadecimal form of the RSVs associated with each code of length i . According to the two lists, the Huffman table can be constructed.

B. Overview of HCM-based RDH Schemes

The previous HCM-based schemes is based on the exploitation of redundancy, which exists in the JPEG bitstream coded with the default Huffman table. The default Huffman table for AC coefficients is provided in the JPEG standard [25], which includes 162 RSVs and corresponding codes. However, for a specific JPEG image, not all the codes appear in the entropy coded data. The symbols/RSVs corresponding to the unused codes have no need to be recorded in HUFFVAL because their frequencies are equal to zero. These symbols are redundant and can be exploited to embed data. The main idea is to replace several unused symbols with one used symbol in HUFFVAL to construct a mapping set between a used code and several unused codes. Each code in a mapping set carries different data. Since the corresponding symbols are the same

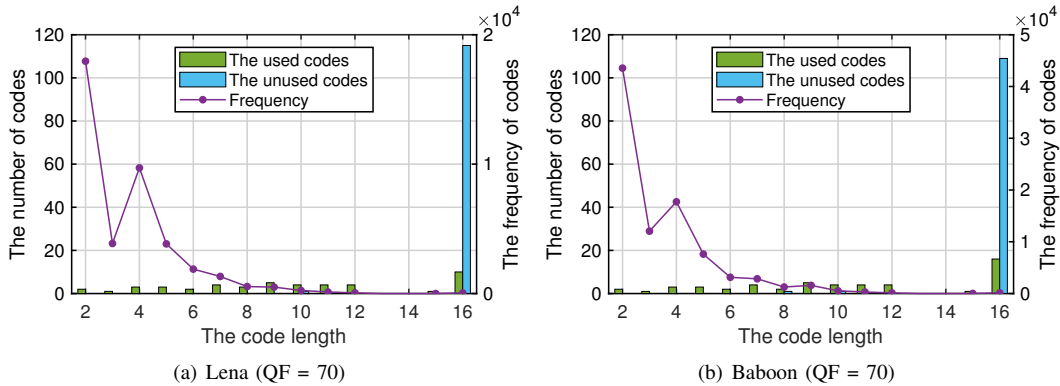


Fig. 2. The statistic results of the Huffman codes on the image "Lena" and "Baboon" with QF = 70.

for all of the codes in a mapping set, the decoded result keeps unchanged after replacing the original code with one of the codes in the mapping set. In addition, the appended bits and codes for the DC coefficients are all unchanged during data embedding. Thus, the HCM-based scheme will not impact the image visual quality.

To keep the file-size unchanged after data embedding, Qian and Zhang [21] proposed to group all the codes according to the code length. Then, the codes in a mapping set are all with the same code lengths. For ease of description throughout the paper, this specific mapping strategy is referred to as grouped-based code mapping (GCM) strategy. The follow-up works [22]–[24] are mainly proposed to improve the embedding capacity by exploiting the statistic information of codes. The adopted mapping strategy is still the GCM strategy proposed by Qian and Zhang [21].

III. MOTIVATION

Although previous HCM-based RDH schemes have satisfying performances on file-size preservation and visual quality, two existing problems cannot be ignored, which are analyzed as follows.

1) *Low Embedding Capacity*: The embedding capacity achieved by the file-size preserving RDH schemes is rather limited compared to HS-based RDH schemes. This is because the limitation of GCM strategy. To demonstrate the statement, we present the calculation of embedding capacity C . Let $\{f_{i,1}, \dots, f_{i,u_i}\}$ denote the frequency of used RSVs in the i -th group, then the embedding capacity EC can be calculated by

$$EC = \sum_{i=1}^{16} \sum_{j=1}^{u_i} f_{i,j} \times \log_2 k_{i,j}, \quad (1)$$

where u_i is the number of used RSVs in i -th group and $k_{i,j}$ is the number of codes assigned for the j -th used RSV in i -th group. The $k_{i,j}$ codes includes $k_{i,j-1}$ unused codes and one used code. According to Eq. (1), the embedding capacity depends on the frequency of used RSVs and the number of unused codes. However, for a JPEG image coded with the default Huffman table, the frequencies of used RSVs assigned with short codes are much larger than the ones assigned with the long codes. Take the typical images "Lena" and "Baboon" as examples, the statistic results are shown in Fig. 2. As depicted in Fig. 2, the frequency of RSV decreases

with the code length increasing and most of the unused codes are with longer lengths. The numbers of unused codes in the first few groups are often near or equal to zero. That means the embedding capacity is mainly contributed by the latter few groups. Thus, the embedding capacity achieved with the GCM strategy is low.

2) *Weak Applicability*: The previous HCM-based schemes can only be applied to the JPEG bitstream coded with the default Huffman table, which exists unused codes. Because the GCM strategy is unavailable when no unused codes exist in the Huffman table. This Huffman table is called as the *optimized Huffman table*, which only includes the used RSVs and corresponding codes.

To address above two existing problems, we propose an adaptive code mapping (ACM) strategy to guide the construction of the mapping relationship. The idea of ACM strategy is that all of the used RSVs are possible to be assigned with multiple unused codes. With the ACM strategy, the RSVs are no need to be grouped according to the code length, which is different from the GCM strategy. The number of codes mapped to each used RSV is unfixed and can be adjusted according to the given constraint. Therefore, the high embedding capacity can be achieved by assigning the high-frequency RSV with multiple codes to construct a mapping set.

In addition, when adopting the ACM strategy to construct the mapping relationship, whether the JPEG encoder uses the default Huffman table or the optimized Huffman table, the Huffman table in the marked JPEG bitstream is only customized according to the frequency of the used RSVs. The unused codes are added according to the constructed code mapping relationship instead of the existing unused codes in the default Huffman table. Therefore, the HCM-based scheme designed based on the ACM strategy is applicable to the JPEG image coded with any Huffman table. That means the applicability is improved compared to using the GCM strategy.

IV. UNIVERSAL FRAMEWORK TO CONSTRUCT THE HCM-BASED RDH SCHEMES

In this section, based on the proposed ACM strategy, a universal framework to construct the HCM-based RDH schemes is proposed. According to the universal framework, the task is to design an optimization algorithm to obtain the optimal

code mapping relationship. Thus, the optimization problems and corresponding evaluation method will be introduced.

A. The Framework

The framework consists of three key modules, which is described as follows:

1) *Bitstream Parsing*: In first, the original Huffman table is constructed by parsing the two lists BITS and HUFFVAL in the DHT segment. With the original Huffman table, all the Huffman codes and appended bits in the entropy coded data are extracted. Then the frequency of used RSVs is counted.

2) *Optimal Code Mapping*: According to a given constraint, the used RSVs are assigned with multiple codes adaptively to construct the optimal code mapping relationship. The optimal code mapping relationship is the one with the best performance under the given constraint. We use a N -dimensional vector to represent the number of codes mapped to different used RSV, such as $\mathbf{m} = (m_1, m_2, \dots, m_N)$. \mathbf{m} is called as the *mapping vector*, where N is the number of used RSVs in the cover bitstream and m_i is the number of codes mapped to the i -th used RSV. The mapping vector \mathbf{m} can be used to represent the mapping relationship. Then, the construction of optimal code mapping can be seen as a *combinatorial optimization* problem, i.e., search the optimal mapping vector under the given constraint. A simple idea is to exhaustive search from the entire solution space, i.e., all the possible mapping vectors and find the one with the best performance. However, it is impractical to evaluate all of the mapping vectors because the solution space is massive. Thus, design a fast and effective optimization algorithm is vital to search for the optimal solution.

3) *Embedding*: With the optimal mapping relationship, the customized Huffman table is constructed by generating the new lists, i.e., BITS and HUFFVAL. The additional data is then embedded by replacing the original code with the one of the codes in a mapping set according to the data to embedded. Other codes are all replaced according to the customized Huffman table. By merging the new file header and new entropy coded data, the marked JPEG bitstream is finally obtained. The marked JPEG bitstream can still be decoded directly by the popular decoders.

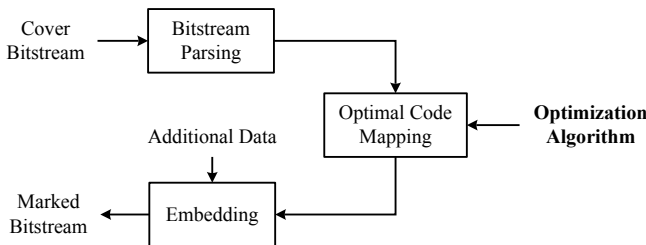


Fig. 3. The universal framework for HCM-based RDH.

The framework is shown in Fig. 3. To construct an HCM-based RDH scheme according to the proposed framework, the key issue is to solve the optimization problem. After designing an effective optimization algorithm to find the optimal solution from the solution space, one can get a new HCM-based RDH scheme for JPEG images.

B. Optimization Problem under Different Constraints

For the marked JPEG image generated by the HCM-based RDH scheme, since the decoded image content is lossless, the optimization of visual distortion is not required. Therefore, the given constraints are generally divided into two categories: payload and file-size increment. Then, the optimization problems can be divided into two types: file-size-limited optimization (FLO) problem and payload-limited optimization (PLO) problem. The FLO problem is to maximize the embedding capacity in the condition that the actual file-size increment is less than or equal to a given increment. Conversely, the PLO problem is to minimize the file-size increment when embedding the data with a given payload.

In fact, optimizing the PLO problem is more valuable than optimizing the FLO problem. In most practical application scenarios, the additional data is first given to perform the embedding process so the given payload is determined. Thus, it is a PLO problem. For the HS-based RDH schemes, the PLO problem is one of the problems to be optimized. Limited to the embedding capacity, for the previous HCM-based schemes, only the FLO problem can be optimized and the optimization is only limited to when the file-size increment is 0. This can explain why the HCM-based RDH schemes are not practical. Based on the proposed universal framework to HCM-based schemes, both of the two problems can be formulated and optimized. Except for the given constraint, two constraints according to the rule of Huffman coding in JPEG standard [25] also need to be considered to define the optimization problems:

- 1) For each used RSV, at least one code should be mapped to it to ensure the correct encoding, i.e., each m_i in the mapping vector $\mathbf{m} = (m_1, m_2, \dots, m_N)$ must be greater than 1.
- 2) The max number of codes in a customized Huffman table can up to 256 according to the JPEG standard [25]. Thus, the sum of m_i is from N to 256. No mapping sets exist in the customized Huffman table when the sum of m_i is equal to N .

Then, the two types of problems are defined as follows:

1) *FLO problem*: For this problem, the given constraint is a specified file-size increment G_I and the optimization objective is to maximize the embedding capacity. Therefore, the FLO problem is formulated as:

$$\begin{aligned} & \max EC(\mathbf{m}) \\ & s.t. \begin{cases} FI(\mathbf{m}) \leq G_I \\ \sum_{i=1}^N m_i \leq 256 \\ m_i \geq 1 \end{cases} \end{aligned} \quad (2)$$

where $FI(\mathbf{m})$ and $EC(\mathbf{m})$ are the file-size increment and embedding capacity for the mapping vector \mathbf{m} respectively. m_i is the i -th element in \mathbf{m} . According to the definition of FLO problem, we can regard the previous HCM-based schemes as the optimization of an FLO problem, i.e., to maximize the embedding capacity under the given file-size increment is 0.

2) *PLO problem*: Opposite to the FLO problem, for PLO problem,, the given constraint is a specified payload G_P

and the optimization objective is to minimize the file-size increment. Therefore, the PLO problem is formulated as:

$$\begin{aligned} & \min FI(\mathbf{m}) \\ & \text{s.t.} \begin{cases} EC(\mathbf{m}) \geq G_P \\ \sum_{i=1}^N m_i \leq 256 \\ m_i \geq 1 \end{cases}, \end{aligned} \quad (3)$$

C. Evaluation of the Mapping Vector

To optimize the two problems, in this section, we introduce the calculation of the embedding capacity and file-size increment to evaluate the mapping vector \mathbf{m} .

1) *Embedding Capacity*: Let $F_{used} = \{f_i^u \mid 1 \leq i \leq N\}$ denote the frequency set of used RSVs in the cover bitstream, the embedding capacity can be calculated directly by

$$EC(\mathbf{m}) = \sum_{i=1}^N f_i^u \times \lfloor \log_2 m_i \rfloor, \quad (4)$$

where $\lfloor \cdot \rfloor$ is the *floor* function.

2) *File-size Increment*: The increment (in bits) in the file-size of the marked bitstream mainly consists of two parts: one is from the DHT segment and another one is from the entropy coded data. Noted that during the bitstream generating, the file size increment caused by byte alignment and zero-byte padding is not included since the increment cannot be predicted in advance and it is so small that it can be negligible.

The increment from the DHT segment FI_{dht} is caused by the extra symbols in the list HUFFVAL to construct the code mapping relationship. One symbol occupies one byte (8 bits) of space in bitstream. We denote the number of symbols in the original Huffman table and the customized Huffman table by N_{ori} and N_{cus} respectively. N_{cus} can be expressed by

$$N_{cus} = \sum_{i=1}^N m_i. \quad (5)$$

Then, the increment from DHT segment FI_{dht} can be represented by

$$FI_{dht} = 8 \times (N_{cus} - N_{ori}). \quad (6)$$

The increment from the entropy coded data FI_{ecs} is caused by code replacing when using the customized Huffman table to generate the marked bitstream. Therefore, FI_{ecs} is equal to the difference of the file-sizes of the entropy coded data in the cover bitstream and the entropy coded data in the marked bitstream. For the entropy coded data, only the Huffman codes for AC coefficients will be modified before and after code replacing. We denote the file-sizes of all the Huffman codes for AC coefficients in cover bitstream and marked bitstream by H_{cover} and H_{marked} . To calculate H_{cover} , the code length for each code is required, which can be parsed from the list BITS in the cover bitstream. Let $L_{cover} = \{l_i^* \mid 1 \leq i \leq 16\}$ denote the number set of codes in different lengths in the cover bitstream and $F_{cover} = \{f_1^*, f_2^*, \dots, f_{N_{ori}}^*\}$ denote the frequency of all RSVs. l_i^* is the number of codes of length i and the sum of l_i^* is equal to N_{ori} . For example, the number of codes of length 3 and 4 are 1 and 3 respectively in Fig. 1.

The code length for each code in the cover bitstream $S_{cover} = \{s_i^* \mid 1 \leq i \leq N_{ori}\}$ can be represented as

$$S_{cover} = \left\{ \underbrace{1, \dots, 1}_{l_1^*}, \underbrace{2, \dots, 2}_{l_2^*}, \dots, \underbrace{16, \dots, 16}_{l_{16}^*} \right\}. \quad (7)$$

Then, the file-size of the Huffman codes in the cover bitstream H_{cover} can be calculated by

$$H_{cover} = \sum_{i=1}^{N_{ori}} f_i^* \times s_i^*. \quad (8)$$

However, the file-size of the Huffman codes in the marked bitstream H_{marked} cannot be calculated directly. Because in the marked bitstream, the number of the codes mapped to all the used RSVs is undetermined and it is possible to exceed 162. That means the list BITS in the marked bitstream needs to be customized. The customization of the list BITS should be based on the frequency of code/symbol instead of the frequency of used RSV. Because the frequency of symbol/code is not equivalent to the frequency of the RSV when the mapping sets exist. In the customized Huffman table, the i -th used RSV is assigned with m_i codes to construct a mapping set. The sum of the frequencies of the m_i codes is equal to the frequency of the i -th used RSV. However, unless the data embedding process is completed, the frequencies of the m_i codes cannot be determined, thereby further generating the list BITS. Paradoxically, the data embedding process can only be performed by first customizing the list BITS. To deal with this, we propose to use the estimated frequency instead of the actual frequency after embedding to customize the list BITS. With the assumption that the "0" and "1" in the additional data are distributed equally, the estimated frequencies of the codes mapped to the i -th used RSV f_i' are the same, which can be represented by

$$f_i' = \frac{f_i^u}{m_i}. \quad (9)$$

It is noted that the estimated frequencies are only involved in the customization of the list BITS so f_i' does not have to be an integer. Then the estimated frequency set F_{est} can be represented by

$$F_{est} = \left\{ \underbrace{f_1', \dots, f_1'}_{m_1}, \underbrace{f_2', \dots, f_2'}_{m_2}, \dots, \underbrace{f_N', \dots, f_N'}_{m_N} \right\}. \quad (10)$$

Take the estimated frequency set F_{est} as input, the list BITS is customized according to the Section K.2 in JPEG standard [25]. To maximize the compression, the high-frequency RSVs should be assigned short codes, which is in accord with the rule of Huffman coding. Therefore, we sort the estimated frequency set F_{est} in descending order and denote f_i'' as the i -th estimated frequency after sorting. In accordance with the customized list BITS, the number set of codes in different lengths in the marked bitstream can be represented by $L_{marked} = \{l_i' \mid 1 \leq i \leq 16\}$. Then, the code length for each code in the marked bitstream $S_{marked} = \{s_i' \mid 1 \leq i \leq N_{cus}\}$

can be expressed as

$$S_{\text{marked}} = \left\{ \underbrace{1, \dots, 1}_{l'_1}, \underbrace{2, \dots, 2}_{l'_2}, \dots, \underbrace{16, \dots, 16}_{l'_{16}} \right\}. \quad (11)$$

Therefore, the file-size of the Huffman codes in the marked bitstream H_{marked} can be estimated as following

$$H_{\text{marked}} = \sum_{i=1}^{N_{\text{cus}}} f_i'' \times s_i'. \quad (12)$$

Then, the increment from the entropy coded data FI_{ecs} can be represented by

$$FI_{\text{ecs}} = H_{\text{marked}} - H_{\text{cover}}. \quad (13)$$

Finally, the total file size for the mapping vector \mathbf{m} can be calculated by

$$\begin{aligned} FI(\mathbf{m}) &= FI_{\text{dht}} + FI_{\text{ecs}} \\ &= FI_{\text{dht}} + H_{\text{marked}} - H_{\text{cover}} \\ &= 8 \times (N_{\text{cus}} - N_{\text{ori}}) + \sum_{i=1}^{N_{\text{cus}}} f_i'' \times s_i' - \sum_{i=1}^{N_{\text{ori}}} f_i^* \times s_i^* \\ &= \sum_{i=1}^{N_{\text{cus}}} (f_i'' \times s_i' + 8) - \sum_{i=1}^{N_{\text{ori}}} (f_i^* \times s_i^* + 8). \end{aligned} \quad (14)$$

V. EXAMPLE: NEW HCM-BASED RDH SCHEME CONSTRUCTED UNDER THE PROPOSED FRAMEWORK

In this section, a new HCM-based RDH scheme is presented as an example of the construction under the proposed framework. In this scheme, an optimization algorithm to automatically search for the optimal solution is provided by adopting the GA, with some problem-oriented designs to improve search accuracy and convergence speed. Then, the details on data embedding and extraction are presented.

A. The Framework of the Proposed GA

Algorithm 1 presents the framework of proposed GA algorithm. In this algorithm, K individuals are random generated to initialize the parent population P . Then, the fitness of each individual in P is computed. To complete the reproduction of new population, the GA operations, i.e., selection, crossover and mutation, are performed to generate the new individuals. The reproduction of new population terminates when the max generation number G_{max} is reached. In the following subsections, some problem-oriented designs in the proposed GA algorithm are introduced.

1) *Encoding for Individual*: To solve the optimization problems using GA, all the tunable parameters in a individual, i.e., the mapping vector $\mathbf{m} = (m_1, m_2, \dots, m_N)$ should be represented with binary encoding. We limit the value of each m_i to be the one in $\{1, 2, 4, 8\}$ to reduce the solution space. Consider the practical applications, that is enough. This limit also can be adjusted. Then each element in $\{1, 2, 4, 8\}$ can be represented by two bits. Such as, the codes "00", "01", "10", and "11" are used to represent 1, 2, 4, 8 respectively. Thus, an

Algorithm 1: Framework of the Proposed GA

Input:

population size K
max generation number G_{max}
crossover rate r_c
mutation rate r_m

Output:

best individual p_{elite}

- 1 Generate initial parent population of K individuals
 $P = \{p_1, p_2, \dots, p_K\}$;
- 2 **for** $i = 1$ to G_{max} **do**
- 3 Compute the fitness of each $p_i \in P$;
- 4 Find the best individual and define as p_{elite} ;
- 5 Insert p_{elite} in the new population P' ;
- 6 Select $K - 1$ individuals from P for reproduction;
- 7 Perform the crossover operation based on r_c ;
- 8 Perform the mutation operation based on r_m ;
- 9 Insert the new $K - 1$ individuals in P' ;
- 10 $P \leftarrow P'$;
- 11 **end**
- 12 **return** p_{elite} ;

individual is composed of a sequence with $2N$ bits. Such as, the t -th individual p_t in the population can be represented by

$$p_t = \{a_i^1 a_i^2 \mid a_i^1, a_i^2 \in \{0, 1\} \text{ and } i \in [1, N]\}. \quad (15)$$

where the pair $a_i^1 a_i^2$ in an individual represents the value of m_i . For example, $a_1^1 a_1^2 = 10$ means the value of m_1 is 4.

2) *GA Operations*: In the reproduction process of the population, we adopt the elite preservation strategy. That is, for the best individual, we insert it in the new population directly instead of modifying it. For the remaining individuals, we use the roulette wheel selection to choose better individuals. After crossover and mutation steps, the generated $K - 1$ new individuals are inserted in the next generation together.

3) *Fitness Computation*: To evaluate the population, the computation of fitness value should be adjusted according to different problems. For the PLO problem, the best individual is the one with the minimal file-size increment, which is calculated according to Eq. (14). However, the roulette wheel selection tends to choose the individual with higher fitness value. Thus, we adjust the fitness value for the t -th individual as follows:

$$\text{fitness}(t) = FI_{\text{max}} - FI_t. \quad (16)$$

where FI_{max} is the maximal file-size increment in one generation and FI_t is the file-size increment caused by the t -th individual calculated by Eq. (14). For the individual that does not satisfy the payload constraint, the fitness value is assigned to 0 as a penalty.

To the opposite, for the FLO problem, the optimization objective is the embedding capacity. Therefore, the fitness is equal to the capacity calculated by Eq. (4). The best individual is the one with the maximal embedding capacity. For the individual that does not satisfy the file-size increment constraint, the fitness value is assigned to 0 as a penalty.

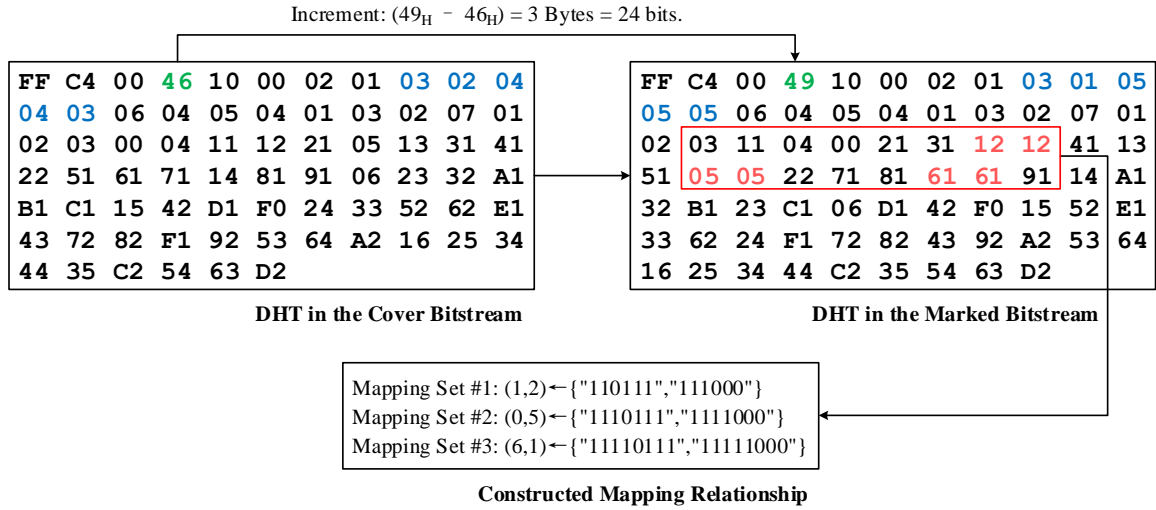


Fig. 4. An example of the modification of the DHT Segment. Compared to the prior HCM-based schemes, the modification on the DHT segment not only includes the symbols in list HUFFVAL, but also the length and the list BITS.

According to the proposed GA, a new HCM-based scheme is constructed under the universal framework. The implementation detail on data embedding and extraction will be introduced in the next section.

B. Implementation Details of Data Embedding & Extraction

After the optimal mapping vector determined, the optimal code mapping relationship can be constructed by modifying the DHT segment. An example of DHT modification is shown in Fig. 4. The DHT segment in the upper left in Fig. 4 is derived from the image "Baboon" at the quality factor (QF) of 70. The DHT segment in the upper right is modified according to the optimal mapping vector produced by our proposed GA under the given payload G_P is 5000. Compared to the DHT segment in the cover bitstream, the file-size of the DHT segment in the marked bitstream increased 3 bytes (24 bits), which caused by the construction of the mapping relationship. The mapping relationship consists of three mapping sets. For each mapping set in Fig. 4, two codes are mapped to one RSV. Therefore three extra symbols have to added in the list HUFFVAL to construct the mapping relationship. The frequencies of RSV "1/2", "0/5", and "6/1" are 2759, 1501, and 748 respectively. Therefore, the embedding capacity is the sum of the three frequencies, i.e., 5008, which is larger than the given payload 5000.

The detailed procedures of data embedding is described below.

- 1) Construct the original Huffman table for AC coefficients by parsing the DHT segment from the cover JPEG bitstream.
- 2) Count all the used RSVs by parsing the entropy coded data according to the Huffman table.
- 3) Find the near optimal mapping vector \mathbf{m}^* according to given objective using the proposed GA described in Section V-A.
- 4) Construct the mapping relationship by modifying the DHT segment in accordance with the mapping vector \mathbf{m}^* .

- 5) Embed the addition data in the entropy coded data by replacing the original codes with one of the codes in a mapping set.
- 6) Merge the modified JPEG header and the modified entropy coded data and then the marked JPEG bitstream is generated.

In the data extraction process, the restored Huffman table has need to be the same with the original Huffman table. We use the optimized Huffman table to synthesize the restored JPEG bitstream. Since the RSV distribution is unchanged after restoring, the restored JPEG bitstream is equivalent to the cover JPEG bitstream. The detailed data extraction steps is described below.

- 1) Construct the customized Huffman table for AC coefficients by parsing the DHT segment from the marked JPEG bitstream.
- 2) Parse the mapping relationship according to the customized Huffman table.
- 3) Extract the embedded data from the entropy coded data according the mapping relationship.
- 4) Synthesize a new JPEG bitstream using the optimized Huffman table.

VI. EXPERIMENTAL RESULTS AND ANALYSIS

A. Datasets

The images tested in our experiments are selected from two commonly used image databases, which are depicted as follows:

1) *USC-SIPI* [26]: The USC-SIPI image database is a collection of digitized images. In our follow-up experiments, four classical 512×512 images from the USC-SIPI image database are selected, namely, "Lena", "Elaine", "Baboon", and "Boat". The four selected images can be classified into two categories. For the first two images, "Lena" and "Elaine", more low-frequency details and smooth areas are contained. On the other hand, more high-frequency details and texture

areas are contained in the second two images, "Baboon" and "Boat".

2) *BOSSbase 1.01* [27]: To further investigate the suitability of the HCM-based scheme constructed by our proposed framework, the popular image database, BOSSbase 1.01, is employed, which consists of 10000 512×512 grayscale images in the PGM format. In our follow-up experiments, 200 images from the BOSSbase image database are randomly selected.

In addition, we convert all the selected images into grayscale JPEG images, since the images in the two databases are uncompressed images. To convert the image from the uncompressed format, TIFF or PGM, into the JPEG format, the `imwrite` function is used in the software MATLAB. All the JPEG images generated by the `imwrite` function is coded with the default Huffman table. To test the suitability of our proposed scheme, the JPEG images coded with the optimized Huffman table are also regarded as the cover images in our experiments. The JPEG images coded with the optimized Huffman table are generated using the `jpeg_read` function and `jpeg_write` function proposed in the JPEG toolbox [28].

B. Evaluation Metrics

For different types of schemes, the evaluation metrics are different, which are as follows:

1) *For HCM-based schemes*: The evaluation metric is the embedding capacity under the zero file-size increment since the prior HCM-based schemes are all the file-size preserving schemes.

2) *For HS-based schemes*: The evaluation metrics include file-size preservation, visual quality, and computational complexity. The file-size preservation and the computational complexity are evaluated using the file-size increment and the running time. For easy comparison, we use the mean square error (MSE) between the cover JPEG image and the marked JPEG image instead of the peak signal-to-noise ratio (PSNR) to evaluate the visual quality. The MSE is represented as

$$MSE = \frac{1}{h \times w} \sum_{i=1}^h \sum_{j=1}^w (X_{i,j} - X'_{i,j})^2 \quad (17)$$

where h and w are the height and width of cover JPEG image. $X_{i,j}$ and $X'_{i,j}$ are the (i, j) -th pixel in cover JPEG image and marked JPEG image respectively. According to Eq. (17), the smaller MSE stands for the better visual quality. When MSE is equal to zero means that the visual quality of the marked JPEG image is no distortion.

In general, the MSE, the file-size increment, and the running time are evaluated under different payloads.

C. Baselines and Experimental Setup

For comparison, two types of recent schemes, i.e., HS-based schemes and HCM-based schemes, are selected as baselines. The selected HCM-based schemes are proposed by including: Qian and Zhang [21], Hu *et al.* [22], and Qiu *et al.* [23]. The selected HS-based schemes are proposed by including: Hou *et al.* [17], He *et al.* [18], Li *et al.* [20], and Yin *et al.* [19].

We have performed the experiments for all the baselines and the proposed scheme on a PC with a 16 GB RAM and

an AMD Ryzen 7 2700 processor with 8 cores. The PC is running with the windows 10 system. The program codes for the schemes proposed by Qian and Zhang [21], Hu *et al.* [22], Qiu *et al.* [23], He *et al.* [18], Li *et al.* [20], Yin *et al.* [19], and the proposed scheme are implemented by ourselves using the software MATLAB and the MATLAB version is R2019b. The program code for the scheme proposed by Hou *et al.* [17] is downloaded from <http://home.ustc.edu.cn/~houdd>.

It is noted that, for prior HCM-based schemes [21]–[23], the cover JPEG images must be coded by the default Huffman table. Because the prior HCM-based schemes cannot be applied to the JPEG images coded by the optimized Huffman table. For a fair comparison, the tested images are all coded by the default Huffman table when comparing with the HCM-based schemes.

For the scheme proposed by He *et al.* [18], the weighting factor α of the negative influence model are set to 0 and 1. $\alpha = 0$ means only the visual distortion is considered so the performance on visual quality is better than other values. $\alpha = 1$ means the performance on file-size increment is better than other values.

For the scheme proposed by Yin *et al.* [19], the cover JPEG images can only be coded by the default Huffman table. Therefore, when comparing with the HS-based schemes, only Yin *et al.*'s scheme [19] is not involved in the evaluation for the performance on the JPEG images coded by the optimized Huffman table.

In this paper, the parameters of the GA in the proposed scheme are determined experimentally, e.g., population size, max generation number, crossover rate, and mutation rate, which is shown in Table. I.

TABLE I
PARAMETERS' SETTING FOR PROPOSED GA.

Parameters	Values
Population size K	100
Max generation number G_{max}	100
Crossover rate r_c	0.8
Mutation rate r_m	0.2

D. Comparison with HCM-based Schemes

The comparison of embedding capacity under zero file-size increment for the four test images from USC-SIPI database is shown in Table. II. The QFs of test JPEG images are set to 10 from 90. It can be observed from Table. II, the embedding capacities achieved by our proposed scheme are almost the highest under different QFs. Compared to [21]–[23], the average capacity of the proposed scheme increases 329.91%-1967.24%, 221.59%-1225.81%, and 184.37%-626.06%, respectively. The reason for the significant improvement compared with the prior HCM-based schemes is the adoption of the customized Huffman table, which is generated according to the frequency of used RSVs of a specific JPEG image. The redundancy is better exploited by our proposed scheme than the previous schemes.

TABLE II
COMPARISON OF EMBEDDING CAPACITY (BITS) UNDER THE CONSTRAINT OF ZERO FILE-SIZE INCREMENT ACROSS QFs FROM 10 TO 90 (FOR THE FOUR TEST IMAGES FROM THE USC-SIPI DATABASE)

Image	Scheme	Quality Factor									Average	Increase(%)
		10	20	30	40	50	60	70	80	90		
Elaine	Qian and Zhang [21]	116	142	177	328	402	218	272	576	1002	359	1967.24
	Hu <i>et al.</i> [22]	341	264	200	414	553	326	409	788	1746	560	1225.81
	Qiu <i>et al.</i> [23]	1036	942	842	933	974	763	781	997	1937	1023	626.06
	Proposed	9894	7438	6300	5776	5905	6461	6347	7996	10717	7426	
Lena	Qian and Zhang [21]	261	210	253	292	365	183	208	249	298	258	1463.91
	Hu <i>et al.</i> [22]	564	326	262	297	370	198	289	352	593	361	1015.56
	Qiu <i>et al.</i> [23]	1253	1004	916	939	996	766	759	695	742	897	349.41
	Proposed	8982	6662	4993	3527	3014	2404	1912	1693	3080	4030	
Baboon	Qian and Zhang [21]	4966	2269	1276	1587	1083	1006	1087	615	342	1581	329.91
	Hu <i>et al.</i> [22]	6596	3475	1760	1792	1274	1312	1363	760	692	2114	221.59
	Qiu <i>et al.</i> [23]	7168	3767	1966	2079	1483	1478	1627	1034	912	2390	184.37
	Proposed	13503	10281	7411	6091	4792	4005	2831	2579	9687	6798	
Boat	Qian and Zhang [21]	484	388	522	481	522	714	370	510	978	552	748.66
	Hu <i>et al.</i> [22]	950	551	691	572	689	811	687	1046	1989	887	428.05
	Qiu <i>et al.</i> [23]	1633	1185	1242	1020	1079	1139	958	1161	2212	1292	262.63
	Proposed	9316	7038	4677	3389	2119	1479	1312	3203	9637	4686	

To demonstrate the suitability of the proposed scheme, the 200 images from the BOSSbase image database are also tested. The average embedding capacities with QF from 10 to 90 are illustrated in Fig. 5. It can be observed from Fig. 5 that the average embedding capacity of proposed scheme is superior than previous HCM-based schemes with any QFs. The capacity decreases with the QF increasing because of the redundancy caused by using the default Huffman table decreases.

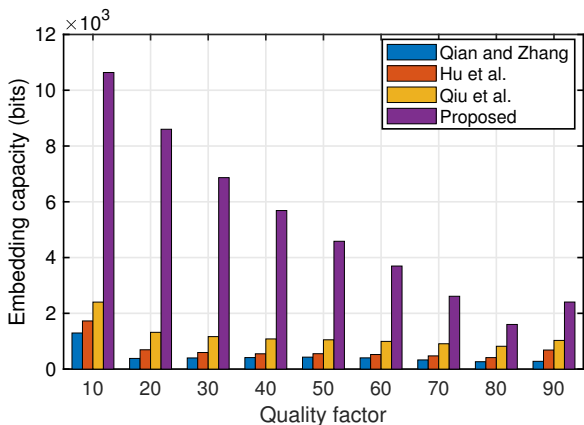


Fig. 5. Average embedding capacity under zero file-size increment of 200 images from the BOSSbase 1.01 image database. The cover JPEG images are coded with the default Huffman table.

E. Comparison with HS-based Schemes

Here, the file-size increment, the MSE and, running time are compared between the HS-based RDH schemes and the proposed scheme. In the first, different payloads are set with different QFs for the four test images from the USC-SIPI database. 2000, 3000, 4000, and 5000 bits of additional data are embedded into the test JPEG images with QF = 30. 3000, 5000, 7000, and 9000 bits of additional data are embedded into the test images with QF = 50. 4000, 7000, 10000, and 13000

bits of additional data are embedded into the test images with QF = 70. 5000, 9000, 13000, and 17000 bits of additional data are embedded into the test images with QF = 90.

1) *File-size Increment*: The file size increments between the cover JPEG images coded with the default Huffman table and the optimized Huffman table are different so they are all evaluated in this experiment.

For the cover JPEG images coded with the default Huffman table, the comparison of the file size increments of the proposed scheme and the previous HS-based schemes is provided in Table. III. The lowest file size increments for different test images with different QFs are displayed in bold in Table. III. It can be observed from Table. III that the file-size increments of all the marked JPEG images generated by our scheme are the lowest. Some file-size increments are even negative, which means that the file-size of the marked JPEG bitstream is smaller than the file-size of the cover JPEG bitstream.

For the cover JPEG images coded with the optimized Huffman table, the comparison of the file size increments of the proposed scheme and the previous HS-based schemes is provided in Table. IV. The lowest file size increments for different test images with different QFs are displayed in bold in Table. IV. It can be observed from Table. IV that most of the file-size increments of the marked JPEG images generated by our scheme are lower than the prior HS-based schemes. Most of the file-size increments of the proposed scheme are a little higher than the given payload while some file-size increments are lower than the given payload. The difference is related to the zero-byte padding and byte-alignment operations in the JPEG standard [25].

Further, we test the performance of file-size preservation on BOSSbase databases. 200 images from the BOSSbase image database are embedded the data with different payloads and different QFs. The average file size increments are shown in Fig. 6 and Fig. 7. The cover JPEG images in Fig. 6 are coded with the default Huffman table and the ones in Fig. 7 are coded with the optimized Huffman table. It is observed from Fig. 6 and Fig. 7 that the average file-size

TABLE III

THE FILE SIZE INCREMENTS (BITS) OF THE MARKED JPEG IMAGES UNDER DIFFERENT QFs AND DIFFERENT PAYLOADS USING THE PROPOSED SCHEME AND THE PREVIOUS HS-BASED SCHEMES. THE INPUT JPEG IMAGES ARE CODED WITH THE DEFAULT HUFFMAN TABLE.

Image	Scheme	Payload (bits) with QF=30				Payload (bits) with QF=50				Payload (bits) with QF=70				Payload (bits) with QF=90			
		2000	3000	4000	5000	3000	5000	7000	9000	4000	7000	10000	13000	5000	9000	13000	17000
Elaine	Hou <i>et al.</i> [17]	3440	4800	6256	7568	4616	7600	10872	13624	6464	10816	14672	18960	7208	13704	20280	26304
	He <i>et al.</i> ($\alpha=0$) [18]	3304	5168	6264	7400	4496	7456	9776	11992	5176	8992	12008	15512	6792	12072	17312	23160
	He <i>et al.</i> ($\alpha=1$) [18]	1752	2888	4056	5520	3008	5664	8120	10816	3480	7072	10464	14520	4144	7760	11976	16536
	Li <i>et al.</i> [20]	1960	2976	4096	5304	3616	5792	8120	10280	5184	8456	11416	14568	6392	11272	16784	22096
	Yin <i>et al.</i> [19]	2640	4048	5360	6848	3776	6440	9632	12656	5160	9120	13440	17432	6872	12776	18632	24944
	Proposed	-5080	-4120	-2976	-1976	-4208	-2064	-120	1960	-3304	-152	2472	5656	-9344	-5312	-1216	2736
Lena	Hou <i>et al.</i> [17]	2728	3784	5136	6664	4296	7008	9552	12424	5808	10080	14032	18176	6568	12208	17640	23648
	He <i>et al.</i> ($\alpha=0$) [18]	2824	4152	5184	6568	4392	6704	9440	12240	5384	9392	13184	17944	6344	10744	16064	21104
	He <i>et al.</i> ($\alpha=1$) [18]	1896	2864	4088	5528	3008	5368	8352	11240	3792	7856	12496	17352	4736	9840	14800	20432
	Li <i>et al.</i> [20]	2048	3400	4736	5928	3288	5616	8256	10896	4336	7736	11384	15688	5360	9408	14304	19072
	Yin <i>et al.</i> [19]	2248	3016	4312	5624	3600	6344	8720	11640	5048	9232	12960	17744	6024	11336	16712	22848
	Proposed	-3936	-2936	-1960	-1040	-608	1288	3320	5264	752	3864	6936	9936	-16	4248	8280	12216
Baboon	Hou <i>et al.</i> [17]	2896	3832	5168	6888	4016	6592	9184	11648	5616	10144	14424	19216	8160	14456	22160	29192
	He <i>et al.</i> ($\alpha=0$) [18]	2888	4040	5384	6520	3696	5856	8240	11840	5688	9632	13904	18672	7784	14272	21912	27920
	He <i>et al.</i> ($\alpha=1$) [18]	1536	2448	3688	4624	2616	4488	7000	9168	4008	6960	11152	15360	5016	9512	14224	19128
	Li <i>et al.</i> [20]	2112	2888	4192	5328	3192	5200	7472	9984	4936	8432	12384	16608	7200	12704	19120	24040
	Yin <i>et al.</i> [19]	2296	3472	4664	5760	3568	5888	8576	11032	5216	9536	13880	18496	7856	13856	21072	27680
	Proposed	-7224	-6088	-5144	-4064	-3176	-1232	824	2656	32	3344	6368	9152	-5072	-912	3152	6896
Boat	Hou <i>et al.</i> [17]	3120	4048	5832	6648	4104	7080	9800	12336	5720	10432	14360	18720	7360	14304	21480	28408
	He <i>et al.</i> ($\alpha=0$) [18]	2928	4184	5272	6408	4232	6544	9480	12232	5784	10272	14328	19264	6384	11952	18272	24760
	He <i>et al.</i> ($\alpha=1$) [18]	1896	3024	4144	5176	2920	5584	8248	11560	4888	8856	13248	17992	5408	10488	15784	21560
	Li <i>et al.</i> [20]	2296	3272	4360	5360	3472	5664	8032	10664	4344	8336	12320	16384	5024	10248	16064	21928
	Yin <i>et al.</i> [19]	2464	3128	4920	5416	3296	5736	8264	11064	4744	9208	13536	17880	6928	12568	19184	25728
	Proposed	-3672	-2616	-1600	-704	-72	1864	3640	5800	1112	3920	7312	10104	-10088	-5784	-1784	2272

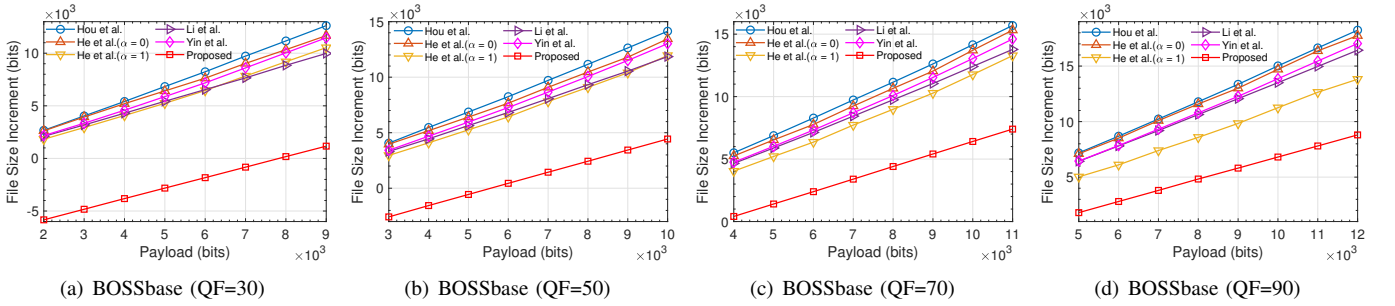


Fig. 6. Average file size increment of 200 images from the BOSSbase image database. The cover JPEG images are compressed by the default Huffman table.

increments obtained by the proposed scheme are lower than the previous schemes at different payloads and QFs obviously. Whether the cover JPEG images are coded with the default Huffman table or the optimized Huffman table, the proposed scheme is effective. Especially for the JPEG images coded with the default Huffman table, the improvement is significant. Except the proposed scheme, the minimal file-size increment is achieved by He *et al.*'s scheme under the weighting factor $\alpha = 1$, which is to minimize the file-size increments.

2) *Visual Quality*: The comparison of PSNR values at different payloads are listed in Table. V. As shown in Table. V, the MSEs of the proposed scheme are always equal to zero. That means the marked JPEG images generated by the proposed scheme keep the visual quality unchanged compared to the cover JPEG images. Also we test the MSEs of the 200 images from the BOSSbase image database. The results are illustrated in Fig. 8. As shown in Fig. 8, the MSEs of the proposed scheme are equal to zero. Among the recent HS-based RDH schemes, Yin *et al.*'s scheme can preserve the best visual quality at any QFs and payloads. For He *et al.*'s

scheme, when the weighting factor $\alpha = 0$, the visual quality is close to Yin *et al.*'s scheme. However, when the weighting factor $\alpha = 1$, the visual quality is poorer than other HS-based schemes. Since only file-size preservation is considered in this case.

3) *Running Time*: For the HS-based RDH schemes, the additional data is embedded by modifying the DCT coefficients, whereas the data is embedded by replacing the codes in JPEG bitstream for our proposed scheme. Since the embedding mechanism is different, the computational complexity cannot be compared and we only compare the running time. The average running time of 50 images from the UCID images database is illustrated in Fig. 9 and Fig. 10. The cover JPEG images in Fig. 9 are coded with the default Huffman table and the ones in Fig. 10 are coded with the optimized Huffman table. As shown in Fig. 9 and Fig. 10, the running time of the proposed scheme is quite lower than the previous schemes. Noted that the running time of Yin *et al.*'s scheme fluctuates obviously, this is because of the computation of the optimization toolbox proposed by MATLAB. It can be

TABLE IV
THE FILE SIZE INCREMENTS (BITS) OF THE MARKED JPEG IMAGES UNDER DIFFERENT QFs AND DIFFERENT PAYLOADS USING THE PROPOSED SCHEME AND THE PREVIOUS HS-BASED SCHEMES. THE INPUT JPEG IMAGES ARE CODED WITH THE OPTIMIZED HUFFMAN TABLE.

Image	Scheme	Payload (bits) with QF=30				Payload (bits) with QF=50				Payload (bits) with QF=70				Payload (bits) with QF=90			
		2000	3000	4000	5000	3000	5000	7000	9000	4000	7000	10000	13000	5000	9000	13000	17000
Elaine	Hou <i>et al.</i> [17]	3368	4584	5504	6632	4896	7624	9832	11952	6560	10720	14216	16936	8864	14672	21176	26192
	He <i>et al.</i> ($\alpha=0$) [18]	3336	4640	5472	6576	4848	7440	9504	11248	5896	10240	13384	16040	8680	14560	20000	25888
	He <i>et al.</i> ($\alpha=1$) [18]	2976	4352	5808	7096	4360	7048	9208	11456	5160	8920	12376	15088	6080	9880	14536	18544
	Li <i>et al.</i> [20]	2832	3848	4984	6400	4776	6672	9504	11704	5624	9144	12744	15968	7448	13144	18864	24648
	Proposed	2032	2960	4008	5048	3136	5064	7128	9080	4120	6856	10104	12936	4840	9096	13592	17072
Lena	Hou <i>et al.</i> [17]	2632	3952	5440	6760	3728	6080	8688	10520	5480	9128	12672	15480	7472	12776	17216	21584
	He <i>et al.</i> ($\alpha=0$) [18]	2576	3832	5328	6760	3616	5808	8768	10656	5424	8944	12192	15648	7680	11776	16840	21168
	He <i>et al.</i> ($\alpha=1$) [18]	2560	4024	5312	6560	3352	5672	8224	10136	5152	8504	11832	15144	6520	10456	15576	19136
	Li <i>et al.</i> [20]	2272	3768	5008	6400	3144	5552	8088	10616	4712	7808	11232	15336	6136	10416	15024	19504
	Proposed	1984	3000	3984	5040	3024	5048	7040	9064	3880	6872	10096	13024	5032	9072	13272	17416
Baboon	Hou <i>et al.</i> [17]	2816	3928	5224	6384	3264	5136	7584	9400	4664	8640	12344	16168	7072	12168	18480	23664
	He <i>et al.</i> ($\alpha=0$) [18]	2888	4072	5288	6360	3080	4960	7320	9832	4736	8344	11968	16352	7776	13512	19864	24624
	He <i>et al.</i> ($\alpha=1$) [18]	1928	2952	4048	5376	2344	4024	6480	8072	3328	6376	9888	13152	4912	8512	12688	16888
	Li <i>et al.</i> [20]	2240	3528	4528	5736	2600	4536	6720	9208	4168	7464	11152	15280	7168	12160	18008	21744
	Proposed	2032	3176	4240	5168	3112	5072	7336	8800	3616	6744	9904	12800	5432	9480	13472	17680
Boat	Hou <i>et al.</i> [17]	2552	3528	4512	5584	3512	5768	7768	9896	4720	8384	11672	14928	7840	14272	19432	24112
	He <i>et al.</i> ($\alpha=0$) [18]	2344	3464	4456	5448	3552	5824	7968	10040	4800	8392	11776	16112	7728	13320	18376	24272
	He <i>et al.</i> ($\alpha=1$) [18]	2104	3304	4376	5504	2888	5256	7640	9816	4048	7352	10536	14184	6648	11144	15552	20168
	Li <i>et al.</i> [20]	2168	3192	4368	5264	3192	5360	7712	9840	4136	7328	11016	14968	6320	11112	17200	21504
	Proposed	2032	3064	4064	5088	3424	4872	6936	8904	3928	6912	10320	13264	5344	9096	13200	17536

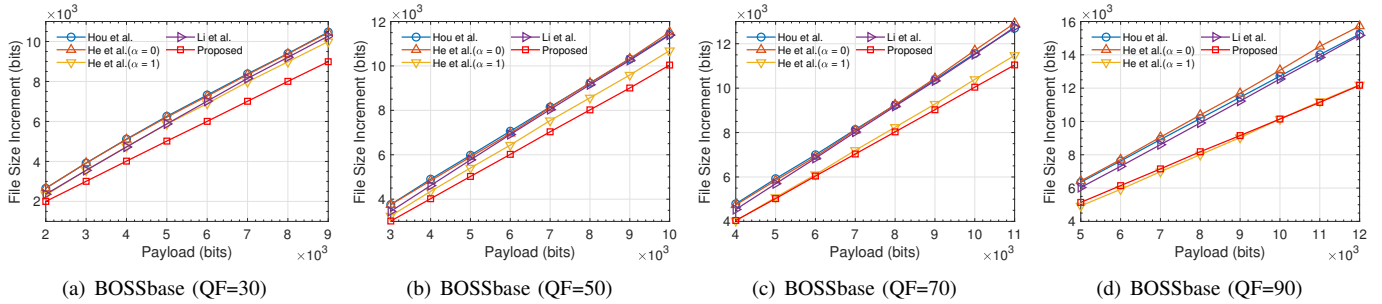


Fig. 7. Average file size increment of 200 images from the BOSSbase image database. The cover JPEG images are compressed by the optimized Huffman table.

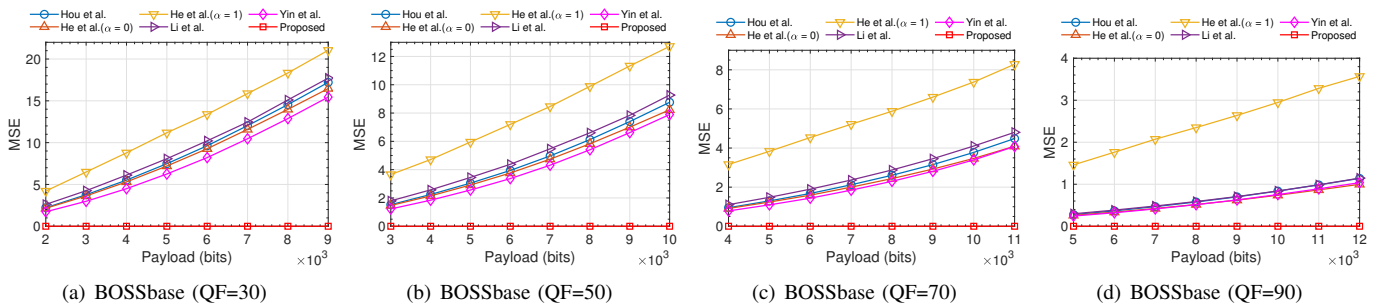


Fig. 8. Average MSE of 200 images from the BOSSbase image database.

TABLE V

THE MSE OF THE MARKED JPEG IMAGES UNDER DIFFERENT QFs AND DIFFERENT PAYLOADS USING THE PROPOSED SCHEME AND THE PREVIOUS HS-BASED SCHEMES.

Image	Scheme	Payload (bits) with QF=30				Payload (bits) with QF=50				Payload (bits) with QF=70				Payload (bits) with QF=90			
		2000	3000	4000	5000	3000	5000	7000	9000	4000	7000	10000	13000	5000	9000	13000	17000
Elaine	Hou <i>et al.</i> [17]	1.81	3.01	4.41	5.99	1.23	2.29	3.54	4.94	0.88	1.69	2.57	3.59	0.40	0.94	1.67	2.54
	He <i>et al.</i> ($\alpha=0$) [18]	1.73	2.97	4.29	5.96	1.15	2.11	3.19	4.45	0.74	1.39	2.11	3.02	0.29	0.60	0.96	1.37
	He <i>et al.</i> ($\alpha=1$) [18]	2.87	4.89	7.79	9.93	1.73	2.85	4.33	5.15	1.29	2.06	2.76	3.56	0.88	1.54	2.02	2.53
	Li <i>et al.</i> [20]	2.34	3.58	5.14	6.87	1.56	2.61	3.85	5.31	0.89	1.61	2.42	3.36	0.30	0.61	0.98	1.38
	Yin <i>et al.</i> [19]	1.52	2.56	3.76	5.29	1.02	1.96	3.11	4.48	0.72	1.46	2.30	3.30	0.37	0.86	1.54	2.35
	Proposed	0	0	0	0	0	0	0	0	0	0	0	0	0	0	0	0
Lena	Hou <i>et al.</i> [17]	2.13	3.69	5.43	7.48	1.31	2.61	4.33	6.41	0.70	1.53	2.60	4.11	0.21	0.42	0.70	1.04
	He <i>et al.</i> ($\alpha=0$) [18]	2.08	3.61	5.38	7.30	1.26	2.54	4.20	6.27	0.66	1.44	2.46	3.95	0.19	0.37	0.59	0.88
	He <i>et al.</i> ($\alpha=1$) [18]	2.88	6.77	8.98	10.17	2.81	5.13	7.90	9.52	1.36	4.11	4.88	6.47	0.79	0.63	1.64	1.12
	Li <i>et al.</i> [20]	2.45	4.31	6.55	9.19	1.50	2.97	5.20	8.38	0.78	1.67	2.99	5.24	0.19	0.37	0.60	0.94
	Yin <i>et al.</i> [19]	1.60	2.60	4.07	5.88	1.02	2.18	3.69	5.76	0.60	1.34	2.34	3.85	0.19	0.38	0.64	0.98
	Proposed	0	0	0	0	0	0	0	0	0	0	0	0	0	0	0	0
Baboon	Hou <i>et al.</i> [17]	2.31	3.90	5.74	7.77	1.79	3.44	5.47	8.04	1.31	2.83	4.86	7.85	0.73	1.62	2.80	4.25
	He <i>et al.</i> ($\alpha=0$) [18]	2.34	4.00	5.81	7.79	1.76	3.44	5.60	7.90	1.27	2.62	4.41	6.80	0.58	1.31	2.34	3.65
	He <i>et al.</i> ($\alpha=1$) [18]	10.96	15.07	17.41	20.77	7.07	14.94	18.98	26.60	8.72	15.47	23.84	31.43	2.21	5.78	9.74	12.91
	Li <i>et al.</i> [20]	2.29	3.85	5.80	7.96	1.73	3.44	5.53	8.10	1.23	2.69	4.74	7.46	0.55	1.24	2.26	3.57
	Yin <i>et al.</i> [19]	2.01	3.37	4.92	6.74	1.57	3.01	4.95	7.50	1.16	2.56	4.62	7.35	0.68	1.51	2.61	3.98
	Proposed	0	0	0	0	0	0	0	0	0	0	0	0	0	0	0	0
Boat	Hou <i>et al.</i> [17]	2.33	3.90	5.66	7.47	1.59	3.16	4.90	6.96	0.89	2.04	3.42	5.14	0.42	0.96	1.60	2.28
	He <i>et al.</i> ($\alpha=0$) [18]	2.28	3.74	5.24	6.92	1.54	3.03	4.73	6.72	0.85	1.97	3.25	4.88	0.24	0.53	0.91	1.39
	He <i>et al.</i> ($\alpha=1$) [18]	4.03	7.56	8.32	10.27	3.88	5.94	10.53	12.57	2.39	5.14	7.44	10.81	1.41	2.66	4.14	4.18
	Li <i>et al.</i> [20]	2.69	4.30	6.04	7.86	1.81	3.45	5.43	7.72	0.97	2.18	3.60	5.54	0.25	0.56	0.97	1.52
	Yin <i>et al.</i> [19]	1.75	2.92	4.54	5.92	1.21	2.51	4.08	6.10	0.75	1.72	3.05	4.81	0.36	0.82	1.39	2.04
	Proposed	0	0	0	0	0	0	0	0	0	0	0	0	0	0	0	0

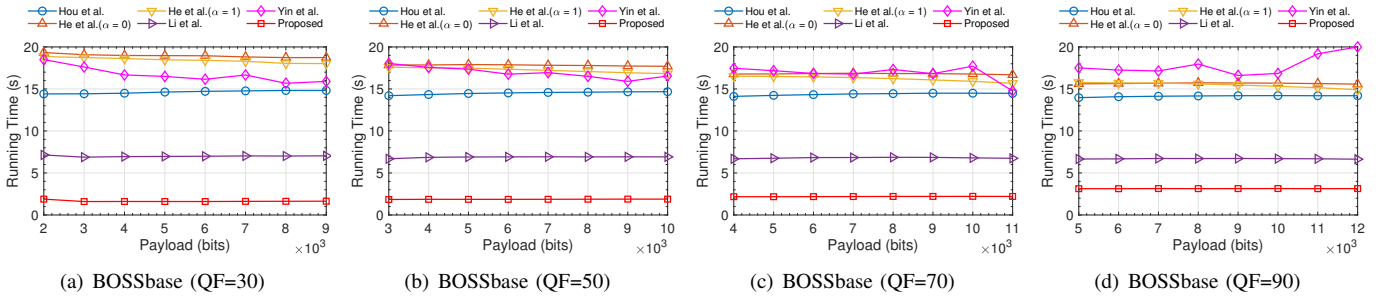


Fig. 9. Average running time of 200 images from the BOSSbase image database. The cover JPEG images are compressed by the default Huffman table.

observed that the runtime of the proposed scheme increases with the QFs increases. That is because the number of nonzero AC coefficients increases and the corresponding codes to be replaced during the bitstream generation are increasing. Thus, more time is required to process the JPEG image. For the HS-based schemes, the number of whole AC coefficients is unchanged under any QF so the runtime is stable. Even if there is an increasing trend in the running time of the proposed scheme, the performance is still better than the other HS-based schemes.

VII. CONCLUSION

As one of the techniques used in RDH for JPEG images, the HCM technique existing two drawbacks, i.e., the low embedding capacity and weak applicability. However, we are attracted by the capability of no visual distortion and thus want to address the two problems. In this paper, we adopt the ACM strategy that each used RSV is possible to be assigned with more than one code. Based on the ACM strategy, we

propose a universal framework to construct an HCM-based RDH scheme for JPEG images. Under the framework, one can get a new HCM-based RDH scheme by designing a specific optimization algorithm. As an example, we propose a new HCM-based RDH scheme using the GA to obtain the optimal code mapping relationship. The proposed scheme can be applied to the JPEG images coded with any Huffman table and obtain the high embedding capacity while keeping the visual quality unchanged. The experiment results demonstrates the performances on both of the file-size preservation and computational complexity of the HCM-based scheme surpass the recent RDH schemes using the most popular technique, HS.

In the future, we will continue to explore the following directions:

- 1) More efficient optimization algorithms can be developed to construct an HCM-based scheme. Under the proposed framework, the design of the optimization algorithm is the only problem to be deal with.
- 2) The performance using the HCM-based scheme on the

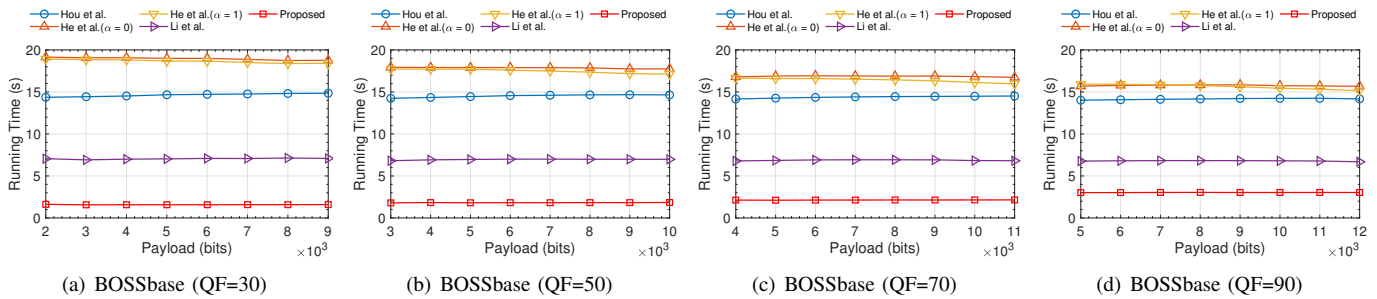


Fig. 10. Average running time of 200 images from the BOSSbase image database. The cover JPEG images are compressed by the optimized Huffman table.

encrypted JPEG bitstream should be investigated. Recently, RDH in encrypted images attracts more and more attention from the researchers, and we are no exception.

ACKNOWLEDGEMENT

REFERENCES

- [1] J. Fridrich, M. Goljan, and R. Du, "Lossless data embedding—A new paradigm in digital watermarking," *EURASIP Journal on Advances in Signal Processing*, vol. 2002, no. 2, p. 986842, 2002.
- [2] M. U. Celik, G. Sharma, A. M. Tekalp, and E. Saber, "Lossless generalized-lsb data embedding," *IEEE transactions on image processing*, vol. 14, no. 2, pp. 253–266, 2005.
- [3] J. Tian, "Reversible data embedding using a difference expansion," *IEEE transactions on circuits and systems for video technology*, vol. 13, no. 8, pp. 890–896, 2003.
- [4] I.-C. Dragoi and D. Coltuc, "Local-prediction-based difference expansion reversible watermarking," *IEEE Transactions on image processing*, vol. 23, no. 4, pp. 1779–1790, 2014.
- [5] Z. Ni, Y.-Q. Shi, N. Ansari, and W. Su, "Reversible data hiding," *IEEE Transactions on Circuits and Systems for Video Technology*, vol. 16, no. 3, pp. 354–362, 2006.
- [6] X. Zhang, "Reversible data hiding with optimal value transfer," *IEEE Transactions on Multimedia*, vol. 15, no. 2, pp. 316–325, 2012.
- [7] W. Zhang, X. Hu, X. Li, and N. Yu, "Recursive histogram modification: establishing equivalency between reversible data hiding and lossless data compression," *IEEE transactions on image processing*, vol. 22, no. 7, pp. 2775–2785, 2013.
- [8] Y. Jia, Z. Yin, X. Zhang, and Y. Luo, "Reversible data hiding based on reducing invalid shifting of pixels in histogram shifting," *Signal Processing*, vol. 163, pp. 238–246, 2019.
- [9] J. Fridrich, M. Goljan, and R. Du, "Lossless data embedding for all image formats," in *Security and Watermarking of Multimedia Contents IV*, vol. 4675. International Society for Optics and Photonics, 2002, pp. 572–584.
- [10] K. Wang, Z.-M. Lu, and Y.-J. Hu, "A high capacity lossless data hiding scheme for jpeg images," *Journal of systems and software*, vol. 86, no. 7, pp. 1965–1975, 2013.
- [11] J. Fridrich, M. Goljan, Q. Chen, and V. Pathak, "Lossless data embedding with file size preservation," in *Security, Steganography, and Watermarking of Multimedia Contents VI*, vol. 5306. International Society for Optics and Photonics, 2004, pp. 354–366.
- [12] G. Xuan, Y. Q. Shi, Z. Ni, P. Chai, X. Cui, and X. Tong, "Reversible data hiding for jpeg images based on histogram pairs," in *International Conference Image Analysis and Recognition*. Springer, 2007, pp. 715–727.
- [13] Q. Li, Y. Wu, and F. Bao, "A reversible data hiding scheme for jpeg images," in *Pacific-Rim Conference on Multimedia*. Springer, 2010, pp. 653–664.
- [14] F. Huang, X. Qu, H. J. Kim, and J. Huang, "Reversible data hiding in jpeg images," *IEEE Transactions on Circuits and Systems for Video Technology*, vol. 26, no. 9, pp. 1610–1621, 2016.
- [15] Z. Qian, S. Dai, and B. Chen, "Reversible data hiding in jpeg images using ordered embedding," *KSII Transactions on Internet and Information Systems (TIIS)*, vol. 11, no. 2, pp. 945–958, 2017.
- [16] F. T. Wedaj, S. Kim, H. J. Kim, and F. Huang, "Improved reversible data hiding in jpeg images based on new coefficient selection strategy," *EURASIP Journal on Image and Video Processing*, vol. 2017, no. 1, p. 63, 2017.
- [17] D. Hou, H. Wang, W. Zhang, and N. Yu, "Reversible data hiding in jpeg image based on dct frequency and block selection," *Signal Processing*, vol. 148, pp. 41–47, 2018.
- [18] J. He, J. Chen, and S. Tang, "Reversible data hiding in jpeg images based on negative influence models," *IEEE Transactions on Information Forensics and Security*, vol. 15, pp. 2121–2133, 2020.
- [19] Z. Yin, Y. Ji, and B. Luo, "Reversible data hiding in jpeg images with multi-objective optimization," *IEEE Transactions on Circuits and Systems for Video Technology*, 2020.
- [20] N. Li and F. Huang, "Reversible data hiding for jpeg images based on pairwise nonzero ac coefficient expansion," *Signal Processing*, vol. 171, p. 107476, 2020.
- [21] Z. Qian and X. Zhang, "Lossless data hiding in jpeg bitstream," *Journal of Systems and Software*, vol. 85, no. 2, pp. 309–313, 2012.
- [22] Y. Hu, K. Wang, and Z.-M. Lu, "An improved vlc-based lossless data hiding scheme for jpeg images," *Journal of Systems and Software*, vol. 86, no. 8, pp. 2166–2173, 2013.
- [23] Y. Qiu, H. He, Z. Qian, S. Li, and X. Zhang, "Lossless data hiding in jpeg bitstream using alternative embedding," *Journal of Visual Communication and Image Representation*, vol. 52, pp. 86–91, 2018.
- [24] C. Zhang, B. Ou, and D. Tang, "An improved vlc mapping method with parameter optimization for reversible data hiding in jpeg bitstream," *Multimedia Tools and Applications*, pp. 1–18, 2020.
- [25] J. Standard, "Information technology—digital compression and coding of continuous-tone still images—requirements and guidelines," *International Telecommunication Union. CCITT recommendation*, vol. 81, p. 09, 1992.
- [26] "The usc-sipi image database," <http://sipi.usc.edu/database>.
- [27] "The bossbase image database," <http://agents.fel.cvut.cz/boss>.
- [28] "The jpeg toolbox," http://dde.binghamton.edu/download/jpeg_toolbox.zip.